Advanced endoscopic imaging of esophageal neoplasia; old looks and new visions

Boerwinkel, D.F.

Publication date
2014

11

OPTIMAL EXCITATION WAVELENGTH FOR PROTOPORPHYRIN-IX FLUORESCENCE OF ESOPHAGEAL ADENOCARCINOMA CELLS AND HUMAN BARRETT TISSUE

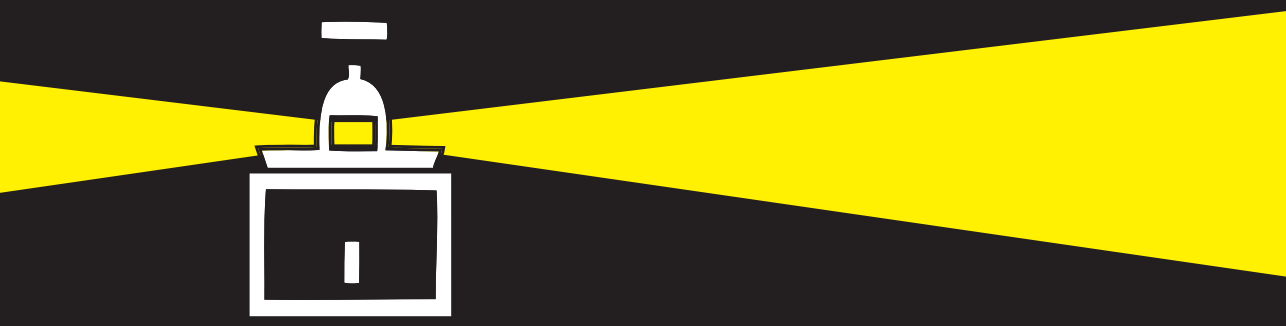

Jasmin A Holz; David F Boerwinkel; Sybren L. Meijer; Mike Visser; Ton G van Leeuwen; Maurice CG Aalders; Jacques JGHM Bergman

Submitted

ABSTRACT

Fluorescence spectroscopy with six wavelengths (369 nm, 395 nm, 400 nm, 405 nm, 410 nm, 416 nm) was performed to determine the optimal excitation wavelength of exogenously induced Protoporphyrin-IX fluorescence in esophageal adenocarcinoma cells and Barrett's esophageal tissue, as this might improve (pre)malignant lesion identification in Barrett's esophagus. Esophageal adenocarcinoma cells OE19 and biopsy specimens from Barrett's esophageal patients were transplanted onto the chorioallantoic membrane of fertilized hen's eggs to simulate the in-vivo situation. Administration of 5-aminolevulinic-acid to the cells/biopsy specimens was followed by sequential fluorescence spectroscopy with all light sources and at several time points between 0 hour before and 28 hours after 5-aminolevulinic-acid administration. Afterwards, the biopsy specimens were histological evaluated and classified. From all obtained emission spectra, the Protoporphyrin-IX fluorescence intensity ratio I636/I600 was calculated to determine the highest intensity ratios and highest difference between short and long wavelengths. Fluorescence spectroscopy was performed on 16 OE19 cell samples and 55 biopsy specimens obtained from 17 patients. Our results suggest that the optimal excitation wavelength for Protoporphyrin-IX in OE19 cells and in Barrett's esophageal tissue lies around 410 nm – 416 nm.

INTRODUCTION

Patients with Barrett's esophagus (BE) are recommended to undergo regular surveillance endoscopy to detect malignant lesions at an early stage. Esophageal adenocarcinoma develops from premalignant stages of dysplasia, which can be detected during endoscopy and graded on histology. These precursor lesions are amendable for curative and minimal invasive endoscopy therapy, due to the virtually absent risk of lymph node metastasis. With a low morbidity and mortality compared to esophagectomy and an excellent 5-year survival rate, the timely detection of early dysplasia is of great clinical importance [1–4]. Existing endoscopic diagnostic procedures such as standard white light endoscopy have a sensitivity and specificity of around 50-80 % [5–9] which shows that today no real time detection tool exists that can clearly discriminate healthy from premalignant tissue during standard surveillance endoscopy. In the absence of visible lesions, random four-quadrant biopsies are obtained throughout the Barrett's segment. This protocol has some drawbacks, such as delayed treatment, high pathology costs and most importantly, sampling errors due to the small surface area, approximately 5% [10], that is sampled within the suspected area.

Early changes in tissue during the progression into malignancy occur at a (sub)cellular level and consist of morphological and chemical changes. All these changes affect the optical absorption and scattering properties of the tissue which can be detected by fluorescence spectroscopy. This approach has shown to be useful to differentiate normal from malignant tissue [11–14]. Photosensitizers, such as 5-aminolaevulinic acid (5-ALA) may be administered to enhance the contrast [15,16]. The administration of 5-ALA bypasses the negative feedback mechanism in the heme biosynthetic pathway and leads to the formation of the fluorescent Protoporphyrin-IX (PpIX). As the conversion of PpIX into heme is a rate limiting step, PpIX accumulates inside the cells with higher concentrations in premalignant tissue [12]. This higher concentration of PpIX increases the fluorescence contrast and may therefore improve the discrimination between dysplastic and non-dysplastic epithelium. This so called photodiagnosis provides real-time information that can be used to red flag areas of interest during medical procedures for the detection of (early) cancer. In previous photodiagnosis procedures broad band light sources were used for the excitation of PpIX. A broad band light source will non-specifically excite all different fluorophores and therefore the emission spectra need to be spectrally resolved to create contrast. Nowadays, new developed laser diodes allow excitation with one wavelength, which can be specifically selected at or close to the excitation maximum of the photosensitizer of interest. This reduces the background fluorescence and may optimize the photosensitizer emission intensity and therefore improve photodiagnosis of different tissue stages. Currently, there is limited knowledge of the optimal excitation wavelength of PpIX in BE tissue.

We hypothesize that by using the optimal excitation and emission wavelength of induced PpIX fluorescence in BE, the contrast between non-dysplastic and dysplastic BE mucosa may be enhanced, thus improving the detection of these early lesions. In in-vitro experiments, dissolved PpIX has a maximal absorption at the Soret band (400-407 nm), in several publications it is shown that the absorption and emission peak maximum and spectral shape depends on

the chemical environment [17–21]. Due to the sharp absorption peak of PpIX a shift of about 10 nm from the Soret band decreases the PpIX absorbance efficiency by around 40 %. Previous experiments with adenocarcinoma cell lines [22] showed cell-specific differences in induced PpIX accumulation. Thus, previous research supports the hypothesis that the PpIX fluorescence intensity is very sensitive to its micro environment and therefore the optimal excitation wavelength might change at different stages of progression toward cancer.

In this study, we used esophageal adenocarcinoma cells as well as human BE biopsies transplanted onto the chorioallantoic membrane (CAM). The CAM model uses the highly vascularized CAM of fertilized hen eggs to keep human cells and small pieces of tissue under similar conditions as in-vivo. Our aim was to study 5-ALA induced PpIX fluorescence to determine the optimal excitation wavelength for PpIX in both, esophageal adenocarcinoma cells and in BE tissue, using a multi-wavelength spectroscopy system consisting of several discrete excitation wavelengths around the 405 nm Soret absorption peak of PpIX.

MATERIALS AND METHODS

Spectroscopy system

A custom made spectroscopy system was developed (2M Engineering Ltd., Veldhoven, The Netherlands), comprising a LED with 369 nm (FWHM of 16 nm) and laser diodes of 395 nm, 400 nm, 405 nm, 410 nm, and 416 nm. The system was connected to an optical fibre probe which delivered the excitation light to the tissue and the fluorescence light back to the connected spectrometer USB4000 (Ocean Optics Inc., Dunedin, Florida, USA) and laptop for spectral recording. The cells/biopsy specimens were placed under the tip of the probe, thus mimicking the in-vivo endoscopic setting.

CAM model

Fertilized hen's eggs obtained from Drost Loosdrecht BV (Loosdrecht, The Netherlands) were incubated for 3 days in a Polyhatch incubator (Brinsea Products Inc., Titusville, Florida, USA) at 38-39 °C, 60-80 % humidity, rotating every 1 hour. At embryonic day 3, a volume of 2-3 mL albumen was removed from the egg using a 21 G needle injected into the air pocket of the egg in order to lower the level of the CAM inside the egg. A window of approximately 1.5 cm was cut into the outer shell on top of the egg in order to gain access to the CAM, using a 10-blade and scissors. After checking the egg was fertilized and the embryo alive, the window was covered with transparent plastic and the egg was placed in a hatcher (Brinsea Products Inc., Titusville, Florida, USA) at 37.5 °C, 50-70 % humidity. The eggs were handled on a heating plate at 37 °C in a laminar flow hood.

Cell line maintenance and transplantation onto the CAM

Human esophageal OE19 adenocarcinoma cells (96071721-1VL, Sigma-Aldrich, St. Louis, Missouri, USA) were cultured in RPMI medium (27016, Gibco, Life Technology Corp., Carlsbad, California, USA) containing 10 % (v/v) Foetal Bovine Serum (10270-106, Gibco) and 1 % Antibiotic-Antimycotic (15240-062, Gibco) at 37 °C and 5 % CO2. At embryonic day 6 of incubation, in preparation of the

cell transplantation, the location on the CAM for cell transplantation was cleaned with dried lens paper previously submerged in ethanol. Subsequently an autoclaved silicon ring was placed on the CAM. A solution of on average 120,000 OE19 cells, dissolved in 40 µL culture medium, was placed into the silicon ring on the CAM. The transparent cover was closed and the egg returned to the hatcher. The cells stayed for 5-9 days on the CAM in order to ensure proper growth.

Patients and biopsy grafting onto the CAM

Patients scheduled for surveillance endoscopy of non-dysplastic BE or work-up or treatment of early Barrett's neoplasia at the department of Gastroenterology and Hepatology of the Academic Medical Center (AMC) Amsterdam were included. The Medical Ethics Committee of the AMC Amsterdam approved the study and all patients were informed and signed a consent form. Biopsies of lesions suspicious for dysplasia within the BE and of endoscopically unsuspicious areas were obtained from 17 patients. Immediately after the biopsies were obtained, they were transferred in preheated 37.5 °C transport medium (DMEM, FCS, PenStrep, L.Glut, Fungizone) and transported to the department of Biomedical Engineering and Physics at the AMC Amsterdam.
At embryonic day 6 of incubation, the egg was placed in the laminar flow hood on a heating plate at 37 °C. The plastic cover was lifted from the egg and the CAM was cleaned at the location for tissue grafting with dried lens paper previously submerged in ethanol. The freshly obtained biopsy specimens were subsequently spread on a gloved finger and with the help of 2 pairs of tweezers carefully spread and placed on the CAM between larger blood vessels. One biopsy specimen was grafted per egg. The transparent cover was closed and the egg returned to the hatcher. The biopsy specimens stayed 2-4 days on the CAM in order to ensure proper attachment.

Spectroscopy procedure

The egg was placed in the laminar flow hoot on a heating plate at 37 °C. The transparent cover was removed and the egg was positioned under the spectroscopy set-up. The optical fibre probe was placed around 1 mm above the cells/biopsy specimen (*Figure 1*), followed by sequential illumination by all light sources and recording of the fluorescence spectra, including a dark measurement (all light sources off). All measurements were performed in a dark room. Subsequently, spectra were recorded adjacent to the cells/biopsy specimen and on the CAM only which was approximately 2 cm from the cells/biopsy specimen. Each saved spectrum was composed of the average of 3 measurements per site. Subsequently, 20 µL of 10 mM 5-ALA (Sigma Chemical Co.) dissolved in 0.9 % NaCl solution was topically administered to the cells/biopsy specimens, followed by fluorescence spectroscopy at several time points between 0 h before and 28 h after 5-ALA administration. After the last measurement, the biopsy specimens were removed from the CAM and fixed in formalin, embedded in paraffin and cut and stained with haematoxylin and eosin (H&E). Histopathological assessment of the biopsy specimens was performed by an expert GI-pathologist. As vital evaluated biopsy specimens were classified into 2 groups, suspicious for dysplasia called 'dysplastic' and not suspicious for dysplasia called 'non-dysplastic'. The cells were not harvested. Finally, the egg was terminated by high dose isoflurane and disposed via the hospital animal waste system.

Figure 1. Fluorescence spectroscopy on biopsy specimen on the CAM.

Data analysis

To compare the PpIX fluorescence intensities and to correct for differences in applied laser power, probe positioning and system performance, the intensity ratio I636/I600 of the PpIX fluorescence peak at 636 nm to a reference emission wavelength at 600 nm was calculated for each spectrum. The mean intensity ratios, the standard deviation (SD), and the standard error of the mean (SEM) were calculated. Statistical relevance of differences in intensity ratios per excitation wavelength and time point were determined by repeated measures one-way ANOVA with subsequent Bonferroni correction using Prism 5 (GraphPad Software Inc., La Jolla, California, USA). The results of the Bonferroni's multiple comparison test were considered significant when the p-value was <0.05. The optimal excitation wavelength was determined by finding the highest intensity ratios and highest difference between short and long wavelengths.

Imaging

Images were obtained from the cells/biopsy specimens on the CAM (*Figure 2*) using a Dino-Lite digital microscope with polarized white light (AM413ZT, AnMo Electronics Corp., Hsinchu, Taiwan) before and after 5-ALA administration. Fluorescence imaging was performed to obtain an overview of the PpIX distribution on the cells, biopsy specimens and CAM. Fluorescence images were obtained at blue light illumination ranging from 400 nm to 430 nm (Crime-lite® 2, Foster + Freeman Ltd., Eversham, UK). A digital camera (Nikon D40X) with a long pass filter (GG455, Foster + Freeman) in front of the lens was used to allow only the detection of emitted fluorescence at longer wavelengths than 435 nm.

RESULTS

Fluorescence spectroscopy at 369 nm, 395 nm, 400 nm, 405 nm, 410 nm, and 416 nm excitation was performed on 16 OE19 cell samples and 55 biopsy specimens, obtained from 17 BE patients, before and after 5-ALA administration.

Figure 3 shows typical emission spectra with subtracted dark spectrum at all 6 excitation wavelengths, 6 hours after 5-ALA administration, of OE19 cells on the CAM (a), a biopsy specimen

(dysplastic) on the CAM (b), the CAM only (c), and the CAM adjacent to the biopsy specimen (d). Fluorescence spectra of OE19 cells and biopsy specimens on the CAM showed equal shapes and PpIX fluorescence peaks at 636 nm emission. Maximum autofluorescence was observed around 500 nm emission. In contrast, the emission spectra adjacent to the biopsy specimens showed negligible autofluorescence and a clear PpIX fluorescence profile. The main difference between

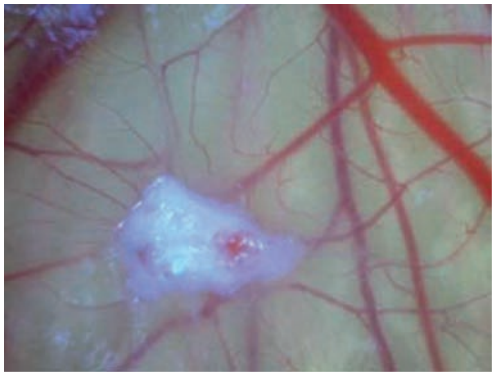

Figure 2. Image of Barrett's esophageal (BE) biopsy specimen on the CAM.

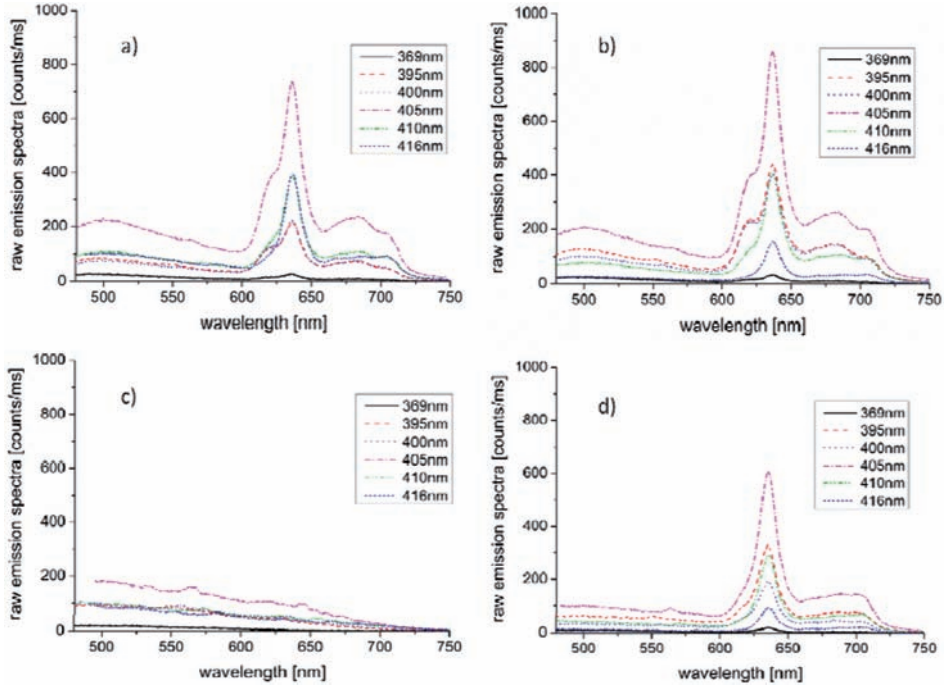

Figure 3. Typical emission spectra with subtracted dark spectrum at all 6 excitation wavelengths, 6 hours after 5-ALA administration, of OE19 cells on the CAM (a), a biopsy specimen (dysplastic) on the CAM (b), the CAM only (c), and the CAM adjacent to the biopsy specimen (d).

the cells/biopsy specimens and the adjacent fluorescence was that the CAM did not show PpIX photoproduct or other porphyrin fluorescence, at 620 nm and 680 nm emission respectively. Fluorescence spectra of the CAM only showed negligible PpIX fluorescence and autofluorescence.

OE19 cells onto the CAM

The PpIX fluorescence intensity ratios I636/I600 at 369 nm, 395 nm, 400 nm, 405 nm, 410 nm, and 416 nm excitation were determined in 16 OE19 cell samples on the CAM before 5-ALA administration at 0 h and at 1.5 h, 4.5 h and 6 h after administration. In addition, 6 of the samples were measured 28 h after 5-ALA administration. All spectra obtained from the OE19 cells, on the CAM adjacent to the cells and from the CAM only were included in the analysis. The intensity ratios I636/I600 at the OE19 cells showed an increasing PpIX intensity with increasing excitation wavelength and increasing time (*Figure 4 (a)*). The Bonferroni's multiple comparison tests of all pairs of time points showed a significant increase in intensity ratios between time point 0 h vs. 4.5 h and 0 h vs. 6 h at all excitation wavelengths except 369 nm. Intensity ratios at 369 nm excitation were significant lower compared to 405 nm, 410 nm, and 416 nm excitation all time points. Intensity ratios at 410 nm vs. 416 nm excitation were not significant different.

Each measurement separately showed that in 94 % (15/16) of all cases, highest PpIX fluorescence intensity ratios were obtained at 410 nm (31 %) and 416 nm (63 %) excitation, 6 h after 5-ALA administration. Lowest intensity ratios were obtained at 369 nm excitation in 81 % (13/16) of the cases. The intensity ratios at 416 nm excitation were 2.3 times higher (SD: ±0.7) compared to 369 nm excitation. The emission intensity peak position of PpIX 6 h after 5-ALA administration was for the OE19 cells on average at a wavelength of 635.8 nm (SD: ±0.5 nm) and showed no dependency on the excitation wavelengths.

The intensity ratios I636/I600 of fluorescence adjacent to the cells (*Figure 4 (b)*), within the ring, showed slower increments compared to cell fluorescence and were significant different in intensity ratios between time point 0 h and 4.5 h as well between 0 h and 6 h at 395, 400, 405, and 410 nm excitation. At 28 h the PpIX fluorescence was decreased to its initial values as before 5-ALA administration. The PpIX fluorescence on the CAM only (outside of the ring, *figure 4 (c)*) showed no significant difference between all time points.

Fluorescence imaging was performed to obtain an overview of the PpIX distribution on the cells and CAM. After 5-ALA administration to the OE19 cells, the fluorescence images (*Figure 5*) showed increasing red fluorescence with increasing time, whereas, before 5-ALA administration, at 0h, no red fluorescence was observed.

Human tissue grafted onto the CAM

A total of 55 biopsies were obtained from 17 Barrett's patients and examined with 5-ALA induced spectroscopy on the CAM. Histological evaluation after retrieval of the transplanted biopsies, classified 18 biopsy specimens as suspicious for dysplasia ('dysplastic') and 12 biopsy specimens as not suspicious for dysplasia ('non-dysplastic'). The remaining 25 biopsy specimens showed intensive necrosis and were therefore excluded from the analysis. Spectra of three as non-dysplastic classified biopsy specimens were excluded from the analysis due to measurement

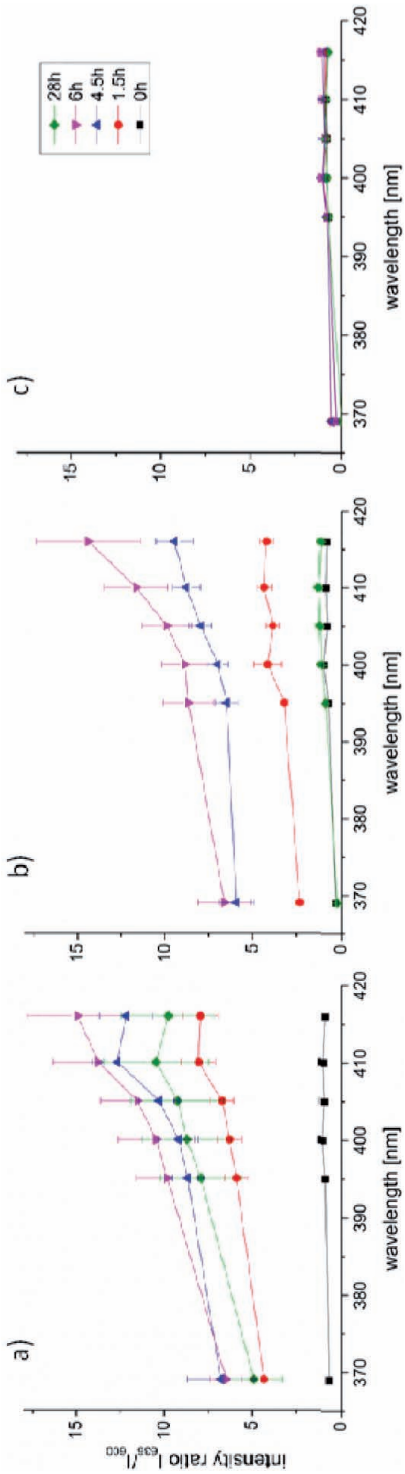

Figure 4. Mean PpIX intensity ratios I636/I600 with standard error of the mean at 0 h, 1.5 h, 4.5 h, 6 h and 28 h after 5-ALA administration obtained from the OE19 cells on the CAM (a), the CAM adjacent to the OE19 cells (b) and the CAM only (c).

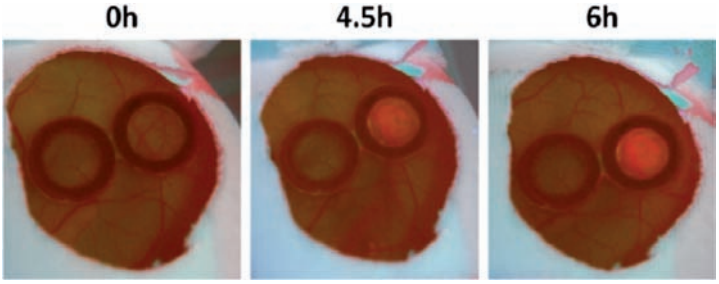

Figure 5. Fluorescence images of the OE19 cells on the CAM. OE19 cells in the rings at 0 h, 4.5 h and 6 h after 5-ALA administration to the right ring (left ring is the control).

issues. *Table 1* gives an overview of the spectra included for the analysis at all six excitation wavelengths obtained from 12 patients.

The PpIX intensity ratios I636/I600 did not differ significantly between dysplastic and non-dysplastic biopsies. Therefore and due to the low amount of biopsy specimens classified as non-dysplastic we decided to analyze all biopsy specimens (*Table 1*) per time point and excitation wavelength in one group, to which we refer further as BE tissue.

The intensity ratios I636/I600 of BE tissue showed increased PpIX fluorescence with increasing excitation wavelength and time point (*Figure 6 (a)*). The Bonferroni's multiple comparison tests of all pairs of time points showed a significant increase in the intensity ratios at 0 h vs. 6 h, 0 h vs. 23 h, 1.5 h vs. 23 h and 4.5 h vs. 23 h at all excitation wavelengths. Intensity ratios at 369 nm excitation were significant lower compared to 405 nm, 410 nm, and 416 nm excitation at all time points. Intensity ratios at 410 nm vs. 416 nm excitation were not significant different.

Each measurement at 4.5 h after 5-ALA administration separately showed that in 96 % (23/24) of the cases, the highest PpIX fluorescence intensity ratios were obtained at 410 nm (63%) and 416 nm (33%) excitation. Lowest intensity ratios were obtained at 369 nm excitation in 96 % (23/24) of the cases. The intensity ratios at 410 nm excitation were 2.3 times higher (SD: ±0.8) compared to 369 nm excitation. The emission intensity peak position of PpIX at 4.5 h after 5-ALA administration for the BE tissue was on average at a wavelength of 635.4 nm (SD: ±1.1 nm) and showed no dependency on the excitation wavelengths or on the classified tissue type's.

The intensity ratios I636/I600 on the CAM adjacent to the BE tissue (*Figure 6 (b)*) tend to increase faster and becomes higher compared to the BE tissue. There was a significant increase of the intensity ratios on the CAM adjacent to the BE tissue between time point 0 h vs. 1.5 h, 0 h vs. 4.5 h, 0 h vs. 6 h and a significant decrease at time points 4.5 h vs. 23 h and 6 h vs. 23 h at all excitation wavelength except 369 nm. At 23 h after 5-ALA administration the PpIX fluorescence was decreased with no significant difference compared to 0 h, before 5-ALA administration. The PpIX fluorescence on the CAM only (*Figure 6 (c)*) increased significant after 6 h, but those intensity ratios were negligible compared to the intensity ratios obtained from the BE tissue or adjacent to it.

Fluorescence imaging was performed to obtain an overview of the PpIX distribution on the BE tissue and CAM. Fluorescence images taken several hours after 5-ALA administration (*Figure 7*)

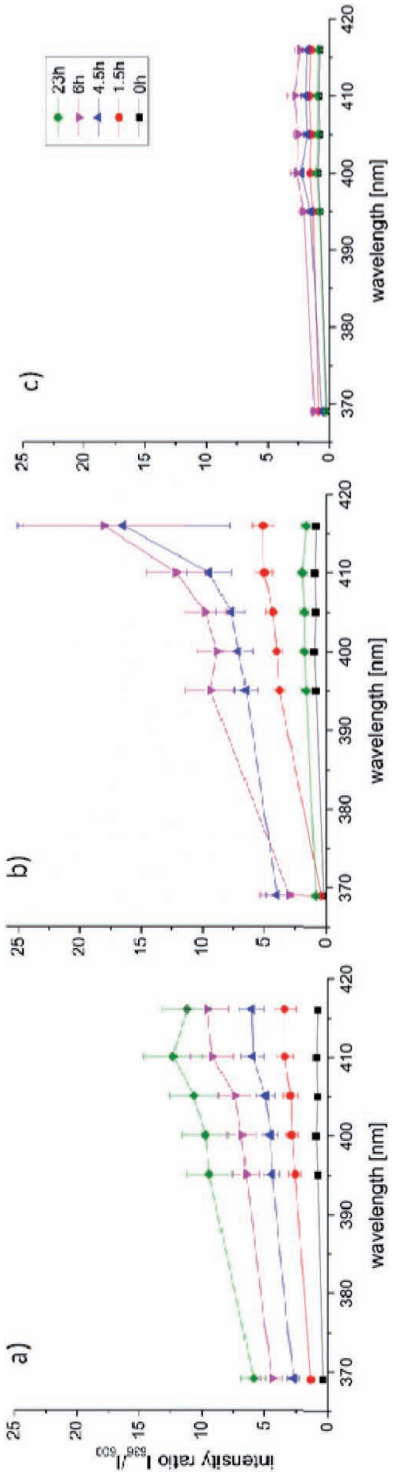

Figure 6. Mean PpIX intensity ratios I636/I600 with standard error of the mean at 0 h, 1.5 h, 4.5 h, 6 h and 23 h after 5-ALA administration obtained from the BE tissue on the CAM (a), the CAM adjacent to the BE tissue (b) and the CAM only (c).

Table 1. Number of analyzed human biopsy specimens on the CAM per time point and their histological classification.

time point	not suspicious for dysplasia	suspicious for dysplasia	sum
0 h	9	18	27
1.5 h	9	18	27
4.5 h	8	16	24
6 h	6	11	17
23 h	2	7	9

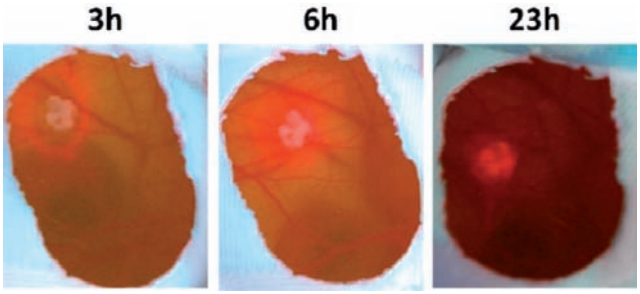

Figure 7. fluorescence images of BE tissue on the CAM. BE tissue (biopsy specimen) at 3 h, 6 h and 23 h after 5-ALA administration.

showed first a high red fluorescence surrounding the BE tissue and with increasing time increasing fluorescence of the BE tissue and decreasing fluorescence of the surrounding CAM.

DISCUSSION

To our knowledge we are the first to graft freshly collected human BE tissue and OE19 cells on the CAM and apply 5-ALA to it. Previous research using the CAM model in combination with 5-ALA focused on tumor specimens and other cell lines [23–26]. The observed conversion into PpIX in our study suggests the existence of a functional metabolism within the cells and BE tissue. This allowed us to determine the optimal excitation wavelength for PpIX in cells and BE tissue, the aim of this study, using a multi-wavelength spectroscopy system and the CAM model. We showed that the PpIX emission intensity depends on the excitation wavelength. As expected, the lowest PpIX intensities were induced with the shortest wavelength 369 nm, which is about 30 nm below the Soret band of PpIX. The optimal excitation wavelength for PpIX fluorescence in OE19 cells and BE tissue was 410 nm and 416 nm without a significant difference between them.

In-vivo, the optimal excitation wavelength of PpIX depends on local environmental factors. Fischer et al. showed a shift in excitation and emission wavelengths between PpIX in solution (methanol/Tris) with a peak emission at 625 nm, whereas in-vivo the PpIX peak shifts to 635 nm [27]. We showed that the emission peak of PpIX around 636 nm in OE19 cells and BE tissue did not depend on the excitation wavelength or on the tissue type and time point.

In our study, the OE19 cells and BE tissue showed increased PpIX fluorescence with increasing time, which is in agreement with known in-vivo observations. The BE tissue showed after 23 hours no significant reduced PpIX fluorescence, which indicates a longer time span for the PpIX clearance compared to in-vivo observations. The fluorescence of the CAM adjacent to the BE tissue showed a faster increase and decrease of induced PpIX, whereas the PpIX fluorescence and autofluorescence of the CAM only showed negligible intensities. Fluorescence images showed that the high PpIX fluorescence adjacent to the cells/biopsy specimens was due to the topical application of 5-ALA surrounding the cells/biopsy specimens.

Although the CAM model was applicable for our research purpose, the spectroscopy measurements had several limitations. The spectroscopy set-up used a mounted probe, to ensure stable measurements. However, due to movements of the embryo and therefore repositioning of the cells/BE tissue under the probe, equal distances and angles of the measurements cannot be assured and sometimes measurements needed to be repeated. Cell measurements showed that the number of used cells were not enough to fill out the entire ring with a multi cell layer. Using a larger amount of cells is recommended. The histological classification showed that 45 % of the grafted biopsies did not stay vital on the CAM and therefore needed to be excluded from the analysis. This suggests the usage of an increased amount of biopsies or to optimize the protocol, for example, by daily administration of growth factors to the BE tissue on the CAM which may prolong tissue vitality.

Differentiation between the OE19 cells, BE tissue and the CAM was possible, due to the differences in spectral shape, 5-ALA kinetics and optimal excitation wavelength. Main difference between cells/BE tissue and the CAM was the PpIX photoproduct and porphyrin fluorescence at 620 nm and 680 nm emission (*Figure 3*), which was not seen on the CAM.

In conclusion, we showed that transplanting esophageal OE19 cells and grafting freshly collected human BE biopsy specimens on the CAM is feasible. This approach allowed determining the optimal optics arrangement for induced PpIX fluorescence. Our results suggest that the optimal PpIX excitation wavelength in OE19 cells and BE tissue lies around 410 nm - 416 nm. Further preclinical research is recommended, with an increased amount of biopsies from non-dysplastic and dysplastic BE tissue, to assess the potential in tissue discrimination.

ACKNOWLEDGMENTS

This research was funded by the 7th Framework Programme for Research and Technological Development, of the European Union, grant agreement number 231993 (EDOCAL).

REFERENCES

1. C. Ell et al., "Endoscopic mucosal resection of early cancer and high-grade dysplasia in Barrett's esophagus," Gastroenterology 118: 670-677 (2000), [doi: http://dx.doi.org/10.1016/S0016-5085(00)70136-3].
2. C. Ell et al., "Curative endoscopic resection of early esophageal adenocarcinomas (Barrett's cancer)," Gastrointest Endosc 65: 3-10 (2007), [doi: http://dx.doi.org/10.1016/j.gie.2006.04.033].
3. A. Behrens et al., "Barrett's adenocarcinoma of the esophagus: better outcomes through new methods of diagnosis and treatment, " Dtsch Arztebl Int 108: 313-319 (2011), 10.3238/arztebl.2011.0313.

4. M. Westerterp et al., "Outcome of surgical treatment for early adenocarcinoma of the esophagus or gastro-esophageal junction," Virchows Arch 446: 497-504 (2005), [doi: http://dx.doi.org/10.1007/s00428-005-1243-1].
5. J. Borovicka et al., "Autofluorescence endoscopy in surveillance of Barrett's esophagus: a multicenter randomized trial on diagnostic efficacy," Endoscopy 38: 867-872 (2006), [doi: http://dx.doi.org/10.1055/s-2006-944726].
6. R. S. DaCosta, B. C. Wilson, N. E. Marcon, "Fluorescence and spectral imaging," ScientificWorldJournal 7: 2046-2071(2007), [doi: http://dx.doi.org/10.1100/tsw.2007.308].
7. W. L. Curvers et al., "Endoscopic tri-modal imaging for detection of early neoplasia in Barrett's oesophagus: a multi-centre feasibility study using high-resolution endoscopy, autofluorescence imaging and narrow band imaging incorporated in one endoscopy system," Gut 57: 167-172 (2008), [doi: http://dx.doi.org/10.1136/gut.2007.134213].
8. W. L. Curvers et al., "Endoscopic tri-modal imaging is more effective than standard endoscopy in identifying early-stage neoplasia in Barrett's esophagus," Gastroenterology 139: 1106-1114 (2010), [doi: http://dx.doi.org/10.1053/j.gastro.2010.06.045].
9. W. L. Curvers et al., " Endoscopic trimodal imaging versus standard video endoscopy for detection of early Barrett's neoplasia: a multicenter, randomized, crossover study in general practice," Gastrointest Endosc 73: 195-203 (2011), [doi: http://dx.doi.org/10.1016/j.gie.2010.10.014].
10. E. R. Tschanz, "Do 40% of patients resected for barrett esophagus with high-grade dysplasia have unsuspected adenocarcinoma?," Arch Pathol Lab Med 129: 177-180 (2005).
11. I. J. Bigio, J. R. Mourant, "Ultraviolet and visible spectroscopies for tissue diagnostics: fluorescence spectroscopy and elastic-scattering spectroscopy," Phys Med Biol 42: 803-814 (1997), [doi: http://dx.doi.org/10.1088/0031-9155/42/5/005].
12. G. A. Wagnieres, W. M. Star, B. C. Wilson, "In vivo fluorescence spectroscopy and imaging for oncological applications," Photochem Photobiol 68: 603-632 (1998), [doi: http://dx.doi.org/10.1111/j.1751-1097.1998.tb02521.x].
13. N. Ramanujam, "Fluorescence spectroscopy of neoplastic and non-neoplastic tissues," Neoplasia 2: 89-117 (2000), [doi: http://dx.doi.org/10.1038/sj.neo.7900077].
14. J. A. Holz et al., "Optimized endoscopic autofluorescence spectroscopy for the identification of premalignant lesions in Barrett's oesophagus," Eur J Gastroenterol Hepatol. 25: 1442-1449 (2013), [doi: http://dx.doi.org/10.1097/MEG.0b013e328365f77b].
15. N. Fotinos et al., "5-Aminolevulinic acid derivatives in photomedicine: Characteristics, application and perspectives," Photochem Photobiol 82: 994-1015 (2006), [doi: http://dx.doi.org/10.1562/2006-02-03-IR-794].
16. B. Krammer, K. Plaetzer, "ALA and its clinical impact, from bench to bedside," Photochem Photobiol Sci 7: 283-289 (2008), [doi: http://dx.doi.org/10.1039/b712847a].
17. L. Brancaleon et al., "Characterization of the photoproducts of protoporphyrin IX bound to human serum albumin and immunoglobulin G," Biophys Chem 109: 351-360 (2004), [doi: http://dx.doi.org/10.1016/j.bpc.2003.12.008].
18. L. Brancaleon, H. Moseley, "Effects of photoproducts on the binding properties of protoporphyrin IX to proteins," Biophys Chem 96: 77-87 (2002), [doi: http://dx.doi.org/10.1016/S0301-4622(02)00035-2].
19. M. Gouterman, G. E. Khalil, "Porphyrin free base phosphorescence," Journal of Molecular Spectroscopy 53: 88-100 (1974), [doi: http://dx.doi.org/10.1016/0022-2852(74)90263-X].
20. J. E. Falk, "Porphyrins and metalloporphyrins; their general, physical and coordination chemistry, and laboratory methods," Elsevier Pub. Co. (1964).
21. V. I. Rakhovski, M. N. Sapozhnikov, A. L. Shubin, "Study of the protoporphyrin luminescence under selective laser excitation," Journal of Luminescence 28: 301-311 (1983), [doi: http://dx.doi.org/10.1016/0022-2313(83)90037-6].
22. H. Brunner et al., "The effects of 5-aminolevulinic acid esters on protoporphyrin IX production in human adenocarcinoma cell lines," Photochem Photobiol 74: 721-725 (2001), [doi: http://dx.doi.org/10.1562/0031-8655(2001)0740721TEOAAE2.0.CO2].
23. C. Hoppenheit et al., "Pharmacokinetics of the photosensitizers aminolevulinic acid and aminolevulinic acid hexylester in oro-facial tumors embedded in the chorioallantois membrane of a hen's egg," Cancer Biother Radiopharm 21: 569-578 (2006), [doi: http://dx.doi.org/10.1089/cbr.2006.21.569].
24. R. Hornung et al., "Systemic application of photosensitizers in the chick chorioallantoic membrane (CAM) model: photodynamic response of CAM vessels and 5-aminolevulinic acid uptake kinetics by transplantable tumors," J Photochem

Photobiol B 49: 41-49 (1999), [doi: http://dx.doi.org/10.1016/S1011-1344(99)00014-7].

25. F. Piffaretti et al., "Real-time, in vivo measurement of tissular pO2 through the delayed fluorescence of endogenous protoporphyrin IX during photodynamic therapy," J Biomed Opt 17: 115007 (2012), [doi: http://dx.doi.org/10.1117/1.JBO.17.11.115007].
26. V. Zenzen, H. Zankl, "Protoporphyrin IX-accumulation in human tumor cells following topical ALA- and h-ALA-application in vivo," Cancer Lett 202: 35-42 (2003), [doi: http://dx.doi.org/10.1016/j.canlet.2003.07.001].
27. F. Fischer et al., "An affordable, portable fluorescence imaging device for skin lesion detection using a dual wavelength approach for image contrast enhancement and aminolaevulinic acid-induced protoporphyrin IX. Part II. In vivo testing," Lasers Med Sci 16: 207-212 (2001). [doi: http://dx.doi.org/10.1007/PL00011356].